

# Application of Fluorescence-Guided Surgery to Subsurface Cancers Requiring Wide Local Excision: Literature Review and Novel Developments Toward Indirect Visualization

Kimberley S. Samkoe, PhD<sup>1,2,3</sup>, Brent D. Bates, MS<sup>2</sup>, Jonathan T. Elliott, PhD<sup>3</sup>, Ethan LaRochelle, BE<sup>3</sup>, Jason R. Gunn, BS<sup>3</sup>, Kayla Marra, BS<sup>3</sup>, Joachim Feldwisch, PhD<sup>4</sup>, Dipak B. Ramkumar, MD, MS<sup>5</sup>, David F. Bauer, MD<sup>1</sup>, Keith D. Paulsen, PhD<sup>3</sup>, Brian W. Pogue, PhD<sup>3</sup>, and Eric R. Henderson, MD<sup>5,6</sup>

## Abstract

The excision of tumors by wide local excision is challenging because the mass must be removed entirely without ever viewing it directly. Positive margin rates in sarcoma resection remain in the range of 20% to 35% and are associated with increased recurrence and decreased survival. Fluorescence-guided surgery (FGS) may improve surgical accuracy and has been utilized in other surgical specialties. ABY-029, an anti-epidermal growth factor receptor Affibody molecule covalently bound to the near-infrared fluorophore IRDye 800CW, is an excellent candidate for future FGS applications in sarcoma resection; however, conventional methods with direct surface tumor visualization are not immediately applicable. A novel technique involving imaging through a margin of normal tissue is needed. We review the past and present applications of FGS and present a novel concept of indirect FGS for visualizing tumor through a margin of normal tissue and aiding in excising the entire lesion as a single, complete mass with tumor-free margins.

## Keywords

near-infrared fluorescence, image-guided surgery, molecular targeting, indirect visualization, sarcoma, ABY-029

Received August 28, 2016. Accepted for publication December 05, 2017.

## Introduction

Application of fluorescence guidance to sarcoma and other subsurface cancers that require negative margins for cure is possible in theory; however, it requires that the cancer's location be monitored indirectly, through its surrounding tissues. Advances such as the clinical development and implementation of near-infrared fluorophores for surgical guidance has allowed for deeper visualization of target tissue due to increased light penetration and reduced tissue autofluorescence; however, the requirement for indirect tumor visualization introduces additional barriers to use of current technology. A recent review by Tipirneni et al highlights the current clinical trials investigating

<sup>1</sup> Department of Surgery, Dartmouth-Hitchcock Medical Center, Lebanon, NH, USA

<sup>2</sup> Geisel School of Medicine, Dartmouth College, Hanover, NH, USA

<sup>3</sup> Thayer School of Engineering, Dartmouth College, Hanover, NH, USA

<sup>4</sup> Affibody AB, Solna, Sweden

<sup>5</sup> Department of Orthopaedics, Dartmouth-Hitchcock Medical Center, Lebanon, NH, USA

<sup>6</sup> White River Junction VA Medical Center, White River Junction, VT, USA

## Corresponding Author:

Kimberley S. Samkoe, Department of Surgery, Dartmouth-Hitchcock Medical Center, 1 Medical Center Drive, Lebanon, NH 03756, USA.

Email: kimberley.s.samkoe@dartmouth.edu



fluorescence-guided surgery (FGS) for the resection of a variety of cancer types.<sup>1</sup> Our research group has undertaken foundational research using a sarcoma-based model through which we hope to define new methodologies to facilitate indirect visualization of subsurface cancers. Here, we outline wide local excision surgery for cancer resection, summarize the development of direct visualization fluorescence techniques, review modern applications of FGS using targeted probes for cancer visualization, and describe our early investigation of indirect tumor visualization utilizing near-infrared fluorescence (NIRF).

### Fluorescence Guidance and Wide Local Excision Surgery for Cancer Resection

The goal in surgery is to effect improvement of the patient's health through a physical intervention that accomplishes one or more of the following: (1) alteration of dysfunctional anatomy, (2) implantation of a device, and (3) removal of an aberrant, harmful structure or tissue. Successful surgery therefore requires the surgeon to correctly distinguish the various tissue types encountered during the operation and to intervene only on the target tissues, leaving the others intact and preferably untouched. This result is not always achieved easily, and numerous technological enhancements to normal surgery have been proposed, one of which is the use of fluorescence guidance.

Fluorescence-guided surgery has proven particularly useful in the removal of brain,<sup>2-5</sup> bladder,<sup>6-8</sup> and head and neck cancers,<sup>9,10</sup> where the tumor is generally present at the organ's surface. These tumors can be visualized directly using fluorescence and can be simultaneously removed in a piecemeal or bulk fashion (Figure 1A-C). However, the application of current fluorescence technology to many other cancers, such as sarcoma, is prevented due to the requirements for complete resection without direct visualization of the mass (Figure 1D-F).

Curative surgery for many cancers requires that the tumor be removed with a zone of normal tissue, called the margin, surrounding the tumor. This is referred to as wide local excision. A tumor removed with no exposed cancer is said to have a "negative margin," while the presence of cancer at the surface of the excised tumor is deemed a "positive margin." Sarcomas, cancers derived from mesoderm—the middle germ layer, are one cancer type that generally requires negative margins for surgical cure. Although a difficult feat with tumors present at an organ's surface, ensuring a negative margin in sarcoma resection is complicated by the subsurface nature of these masses, requiring surgeons to accurately estimate the precise location and distance of the tumor surface from their dissection without directly visualizing the mass. This is not always achieved easily and frequently results in positive margins, which are associated with increased local recurrence and lower survival rates.<sup>11-14</sup> Unfortunately, resection of sarcoma tumors results in positive margins in approximately 22% to 34% of cases, as reported in three large series.<sup>11-13</sup>

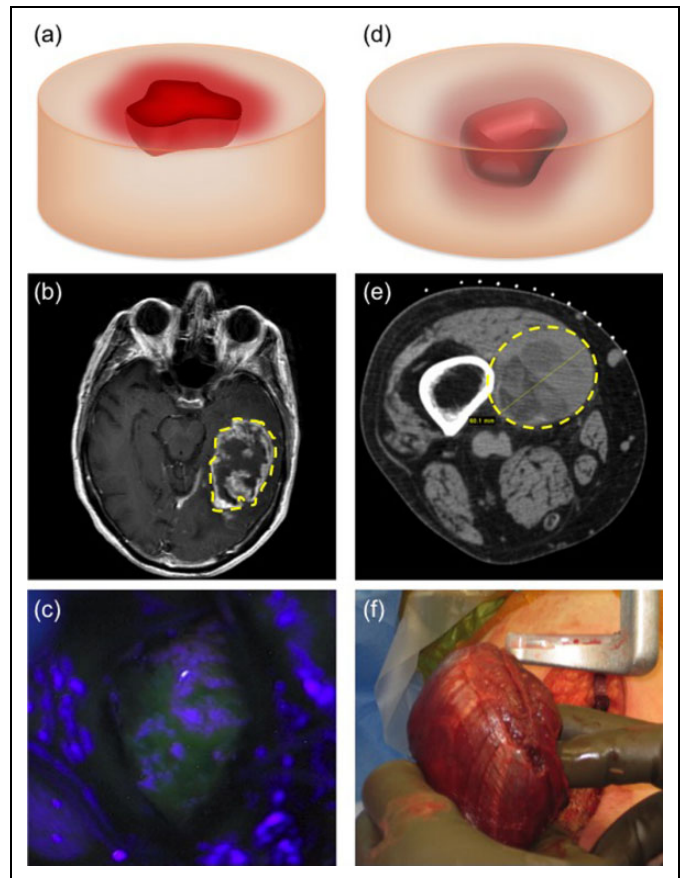


**Figure 1.** A, Concept of direct fluorescence-guided surgery (FGS), in which the tumor is present at the organ's surface and can be visualized directly using an intraoperative fluorescence microscope. B, Anticipated resection of a glioma tumor as seen on brain magnetic resonance imaging (MRI; dashed yellow line). C, Intraoperative view of a glioma tumor as seen with direct fluorescence visualization after administration of 5-aminolevulinic acid (ALA). D, Concept of indirect FGS, in which fluorescence is utilized to display tumor location and depth through a margin of normal tissue. E, Anticipated resection of a soft-tissue sarcoma on computed tomography (CT; dashed yellow line). F, Intraoperative photograph of a soft-tissue sarcoma that has been removed with a margin of muscular tissue surrounding the tumor.

Fluorescence guidance during wide local excision of sarcoma tumors is a strong candidate for future applications and may improve primary resection of other subsurface tumors. However, there is clinical need for a novel technique to allow surgeons to visualize and monitor tumor through a margin of normal tissue.

### Historical Overview of FGS

Given the importance of surgical margins in predicting recurrence and outcome in many solid tumors, the idea that fluorescence can be used for in situ tumor differentiation has captivated clinicians and researchers alike. Although early reports of in vivo fluorescence use dates to at least 1948, when Moore et al reported the use of fluorescein sodium (FS) as a

tool for surgical resection of brain tumors,<sup>15</sup> intraoperative techniques have only gained wider adoption since the 1990s. Analogous to FS, indocyanine green (ICG), which originated in ophthalmology for retinal angiography, has also been utilized as a vascular tracer in neurosurgery. Both of these agents are readily available, and widespread adoption can be attributed mainly to their status as approved Food and Drug Administration (FDA) drugs that are then used off-label for FGS. As vascular tracers, FS and ICG extravasate in brain regions where the blood–brain barrier is compromised, allowing for the discrimination of tumor tissue over normal tissue. However, a major limitation of these tracers is that they rely exclusively on the enhanced permeability and retention (EPR) effect as the driver of contrast. Due to their affinity to bind to albumin, they have an effective molecular weight of >100 kDa and thus remain primarily in the blood. As a result, in regions of the infiltration margin where blood–brain barrier disruption has not yet occurred, tumor contrast is limited and variable, ultimately reducing the efficacy of these agents. Nevertheless, they have been adopted for use in lung, head and neck, breast, colorectal, melanoma, gastric, endometrial, and prostate cancer resections, and there are currently 54 active and recruiting studies listed on ClinicalTrials.gov using these two agents.

Due to the enormous costs of drug development, FGS would continue to be limited to off-label use of already approved agents. In 1999, the FDA approved the use of 5-aminolevulinic acid (ALA) for the treatment of actinic keratosis by photodynamic therapy. Because ALA also induces the accumulation of protoporphyrin IX (PpIX) in certain tumor cells (due to its naturally occurring presence as a precursor to PpIX in the heme synthesis pathway), Stummer et al were able to demonstrate its use as a highly specific marker of high-grade glioma tissue.<sup>2</sup> Their seminal paper in *Lancet Oncology* in 2006 showed an improvement in the number of patients with 6-month progression-free survival (from 21% to 41%) with the use of ALA during glioma surgery.<sup>2</sup> Subsequent papers by groups at the University of Toronto and Dartmouth College<sup>3,16,17</sup> have refined the broad strokes of Stummer et al, characterizing the use of ALA in low-grade gliomas and other brain tumors, as well as advancing mechanistic understanding through preclinical research.

Although the surgical use of ALA continues to be investigated in at least 50 studies listed on ClinicalTrials.gov, it is generally understood that for brain tumors, ALA provides excellent visual contrast in high-grade gliomas, but low-grade gliomas require quantitative imaging or sensing techniques to differentiate between normal and diseased tissues.<sup>3,17</sup> It is likely that both reduced EPR and reduced downregulation of ferrochelatase associated with low-grade or marginal glioma cells contribute to the reduced sensitivity of ALA in these cases. Furthermore, anecdotal evidence from Dartmouth's experience, corroborated by preclinical results,<sup>18</sup> suggest that ALA can enhance normal tissue in certain cases and that concurrent therapies such as dexamethasone can influence the degree of background enhancement associated with ALA. These observations limit the applicability of ALA and have

resulted in further exploration of imaging agents for use in FGS.

In recent years, there has been a strong push by a number of groups to develop more specific tumor-enhancing fluorescent agents to overcome certain limitations of current agents, which are mainly limited to FS, ICG, ALA, and methylene blue. Neurosurgical applications represent the knife-edge of translational development, but applications in head and neck surgery have also introduced new agents in the past 5 years. Although drug development costs remain an obstacle, the introduction of good manufacturing practice (GMP)-produced near-infrared fluorophore IRDye 800CW (LI-COR Biosciences, Inc, Lincoln, Nebraska),<sup>19</sup> as well as microdose exploratory investigational new drug (eIND) pipelines by Dartmouth<sup>20,21</sup> and other groups, has spurred development. In the next section, we will review the targeted agents that have been developed in the last 5 years for FGS applications and highlight the ongoing and future clinical trials at Dartmouth College.

## Modern Applications of NIRF for Targeted Probe Surgical Guidance for Cancer

### Neurosurgery

Intraoperative ALA continues to be the most important tool for high-grade glioma resection guidance and is standard of care for several European countries.<sup>4</sup> In terms of clinical acceptance, there is level I evidence showing the efficacy in World Health Organization III and IV grade gliomas. Perhaps more importantly, ALA has been readily adopted by surgeons because it is specific and sensitive within the context of high-grade gliomas and can be visualized directly using an operating microscope equipped with standard filters. Fluorescence-guided surgery research and development have centered on expanding the types of tumors for which detectable contrast can be measured and, pursuant to that, improving the means of detection over direct visualization. Pioneering work at the University of Toronto and Dartmouth College has refined probe-based and quantitative wide-field imaging systems,<sup>3,16,17</sup> to the point where 0.01 (17.8 nM) and 0.1 µg/mL (178 nM) concentrations, respectively, can be readily detected. As device sensitivity increases, tumor enhancement becomes more detectable, while background enhancement (false positive) is readily reduced.

BLZ-100, a synthetic peptide ICG derivative conjugate (Blaze Bioscience, Seattle, Washington), was the first targeted fluorophore to enter phase I clinical trials.<sup>5,22</sup> The conjugate is a 36-amino acid sequence isolated from the venom of the scorpion, *Leiurus quinquestriatus*, and has demonstrated tumor-specific activity mainly through annexin A2 binding. The clinical motivation for BLZ-100 development has been pediatric brain cancer, although the company has completed proof of principle and preclinical studies examining several types of cancer including pediatric glioma, head and neck, sarcoma, breast, and skin cancer. BLZ-100 has demonstrated strong contrast in preclinical studies between tumor and normal

tissue, and toxicology studies have been completed in rats and monkeys with promising results.<sup>5,23</sup> Clinical trials to determine the efficacy of BLZ-100 are currently underway for several cancer types.

A 2013 study by Sexton et al compared IRDye-labeled cetuximab and IRDye-labeled anti-epidermal growth factor receptor (anti-EGFR) Affibody molecules (Affibody AB, Solna, Sweden) and found that the smaller Affibody-based dyes penetrated through the blood-brain barrier and provided better enhancement in the peripheral tissue.<sup>24</sup> This finding led the researchers to develop a GMP production pipeline to manufacture a compound consisting of IRDye 800CW conjugated to synthetic anti-EGFR Affibody, subsequently called ABY-029, for preclinical toxicology and efficacy studies, followed by a first in-human clinical trial (NCT0291925).<sup>20,21</sup> The pipeline crystallized around the idea that microdoses of synthetic peptide conjugate could be administered to patients under an eIND, avoiding the need for multispecies toxicology studies. Consequently, for successful imaging of microdose-level (30 nanomoles) fluorescence, there were several requirements: (1) the receptor of interest must be expressed in abundance, (2) the fluorophore must be excited by a powerful wide-field light source at close to peak absorption wavelength, and (3) the remitted signal must be detected by a sensitive, cooled scientific complementary metal-oxide semiconductor (CMOS) camera.<sup>25</sup> Other considerations included the need for highly specific binding with low background signal and fast plasma clearance to allow imaging 1 to 4 hours postinjection with good contrast. In 2016, Samkoe et al published toxicology results for ABY-029 with an absence of significant adverse effects at 1000× the microdose level,<sup>20</sup> and in a subsequent study, favorable contrast ratios were identified at early imaging time points (1-48 hours).<sup>26</sup> Furthermore, simultaneous injection of ABY-029, PpIX, and low-molecular-weight IRDye 680RD-CX (LICOR Biosciences, Inc) showed that for EGFR-positive tumors, ABY-029 had higher tumor contrast than PpIX or perfusion dye (IRDye 680RD-CX) and that combining ABY-029 and PpIX information provided better discrimination between tumor and normal brain than either alone. Interestingly, the efficacy of this dual tracer method was found in both EGFR-positive and EGFR-negative tumors.<sup>27</sup> ABY-029 is currently being investigated in a first in-human clinical trial, and additional preclinical work is underway to further investigate the potential application of this molecule toward brain and other types of cancer.

### Head and Neck Surgery

Successful surgical resection of head and neck squamous cell carcinomas (HNSCC) depends on a careful balance between obtaining clear surgical margins and maintaining physiological function and cosmetic appearance of pertinent structures in the facial region and oral cavity. The current clinical standard of care for HNSCC margin determination is gross palpation during surgery and confirmation of clear margins with pathological tissue staining; however, microscopic tumor burden at or

near the surgical margins remains high and recurrence of these patients approaches 40%.<sup>28</sup> Several studies involving ICG have been undertaken for the detection of tumor margin boundaries and sentinel lymph node detection. Indocyanine green is a nonspecific perfusion fluorophore and, as such, determination of tumor boundaries depends on the differential uptake and clearance kinetics in normal and diseased tissues, ultimately resulting in poor tissue delineation.<sup>10</sup> However, ICG plays a much more promising role in the detection of sentinel lymph nodes, where passive uptake and retention are a feature of pathological lymph node detection, and the near-infrared detectability lends to deeper node imaging.<sup>10</sup>

Recently, fluorescently labeled molecular targeting agents for HNSCC resection have gained momentum to better target tumor versus normal tissue and to visualize both bulk and microscopic tumor burden. The Rosenthal group has pioneered work in near-infrared imaging of EGFR-targeted antibodies.<sup>9,29-35</sup> Cetuximab and panitumumab have both been independently conjugated with IRDye 800CW and are in active clinical trials (NCT01987375 and NCT02415881, respectively) for HNSCC detection and surgical removal. However, at short time periods, antibody-based imaging agents generally had confounding signal in normal tissues resulting in low tumor-to-background ratios (TBRs) or tissue contrast. To overcome this limitation, extensive clearance times (>48 hours) are used, where internalization and cell cycling dominate the signal but provides promising TBRs approaching 5:1.<sup>9,35</sup> To further increase TBRs, simultaneous injection of unlabeled cetuximab much larger than the fluorescent dose (a “cold-dose”) is being tested to overwhelm endogenous EGFR sinks and increase the observed contrast by maintaining higher levels of circulating fluorescent antibody.<sup>35</sup>

The recent development of GMP-produced IRDye-labeled anti-EGFR Affibody molecule, ABY-029, has spurred interest in head and neck surgery. A clinical trial of ABY-029 in HNSCC resection was recently approved at our institution (NCT03282461), and it is possible that this Affibody compound may represent a superior alternative to the larger antibody-based compounds cetuximab and panitumumab. However, improvement in long-term survival will be determined from the ongoing and future clinical trials, and further investigation is likely required to delineate the optimal technique for fluorescence-guided HNSCC resection.

### Orthopedic Surgery

Fluorescence applications in orthopedic surgery are less developed than in many other medical disciplines. One reason for slower progress stems from the fact that the most common tissue target for orthopedic surgeons, bone, is generally characterized well with conventional radiographs, which can be employed on-demand during surgery. Other imaging modalities such as computed tomography (CT) and magnetic resonance imaging (MRI) are also readily available and can provide detailed and reliable anatomical data. A second reason is that the rigidity of bone provides an unambiguous

tactile reference point with landmarks that are consistent across patients. Finally, orthopedic operations for cancer, the greatest impetus for molecular guidance in other surgical specialties, comprise an exceptionally small proportion of all orthopedic procedures. Still, molecular-guided fluorescence imaging is being explored increasingly in orthopedics, especially with reference to surgical removal of primary bone and soft-tissue sarcomas.

The area of most study for orthopedic oncologic fluorescence applications is the detection of residual cancer cells at the time of primary tumor resection. In 2012, Mito et al published an important manuscript detailing the successful use of a cathepsin-activated fluorescent probe for detection of residual cancer cells following the removal of soft-tissue sarcomas in a mouse model.<sup>36</sup> Detection of residual disease had a positive association with disease recurrence, and the authors were able to demonstrate reduced local recurrence with real-time fluorescence-guided removal of residual tumor cells. The same group later published a first-in-human phase I clinical trial (NCT01626066) using a protease-activated fluorescent probe (LUM015; Lumicell Inc, Wellesley, Massachusetts) and demonstrated safe administration and tumor-specific labeling in soft tissue sarcomas.<sup>37</sup> A second group recently published a series of studies demonstrating that the use of a telomerase-dependent adenovirus fluorescent probe (OBP-401; Oncolys BioPharma Inc, Tokyo, Japan) during surgery improves tumor resection, reduces local recurrence, and improves disease-free survival in murine models of osteosarcoma, retroperitoneal fibrosarcoma, and soft tissue sarcoma.<sup>38-41</sup> These data indicate the potential clinical utility of FGS in reducing recurrence rates of certain musculoskeletal tumors.

Similar to prior work in neurosurgery and otolaryngology, the work of these two groups relies on direct, superficial recognition of cancer cells.<sup>36-41</sup> Although real-time detection of residual cancer cells offers an immense improvement over current surgical methods, avoiding residual cancer altogether would be more desirable. However, for reliable wide local excision with negative margins, definition of new fluorescence applications will be required in order to transition to indirect tumor visualization through marginal tissues. Here, we introduce the foundational fluorescence work required to develop indirect FGS using a sarcoma model. Furthermore, we have initiated a phase 0 clinical trial investigating ABY-029 in primary sarcoma tumors (NCT03154411).

## Proposed Future Uses of NIRF for Indirect Visualization: Foundational Fluorescence Work

### Description of Applications

Curative surgery for sarcoma requires that the tumor be removed with a margin of normal tissue surrounding the lesion. However, accurate localization of a cancer through its surrounding tissues and estimation of margin thickness will

require a model that accommodates for numerous factors. These include: (1) energy of the excitatory signal, (2) tumor volume, (3) tumor fluorophore uptake, (4) tumor optical characteristics, (5) surrounding tissue thickness before dissection, (6) surrounding tissue fluorophore uptake, (7) surrounding tissue type(s) and optical characteristics, and (8) presence and effects of preoperative cancer therapies on the tumor and surrounding tissue optical properties. These important factors are knowable prior to surgery through the use of three-dimensional imaging (MRI and/or CT) and analysis of the tumor's optical properties at the time of diagnostic biopsy. This would require the intended fluorescent probe to be administered at the time of biopsy so that the tumor's probe uptake could be assessed. The near-infrared EGFR-targeted probe ABY-029 is an excellent candidate as the excretion kinetics are fast, and preliminary work suggests that optimal TBR contrast occurs within hours, compared to days as in the case of antibody-conjugated molecules.<sup>26</sup> In addition, tissue autofluorescence is minimized in the near-infrared region, further enhancing tumor contrast and facilitating accurate indirect tumor visualization. Finally, the GMP form of ABY-029 has been rigorously tested for toxicity<sup>20</sup> and as a targeted agent in paired-agent imaging of several EGFR-expressing cancers<sup>42-44</sup> and is currently approved for human testing through the FDA eIND #122681.

Because the development of a surgical model requires reproducible working conditions for numerous serial experiments, we chose to begin delineating these optical properties in a tissue-simulating phantom model<sup>45</sup> using well-described scattering and absorption parameters.<sup>46,47</sup> We then transitioned our work to a naive rodent model for *in vivo* validation in normal tissues. Finally, we tested the ability of a surgeon, blinded to the location of a tumor-simulating inclusion, to successfully isolate the inclusion with ~1 cm margins using a preclinical surgical imaging system.

## Materials and Methods

### Well Phantoms

Molds were created by drilling holes with 5 mL volume (19 mm diameter, 17 mm depth) into black Delrin<sup>®</sup> plastic. Powder gelatin (10% wt/vol) was mixed in hot water, stirred vigorously until cooled to 30°C, and infused with 50 nM of IRDye 800CW. Varying concentrations of blood and intralipid were added to the gelatin mixture, and then the mixtures were poured into the appropriate wells. The rows had varying blood concentrations (0.5%, 1%, and 2% vol/vol) as an absorbing agent, and the columns had varying intralipid concentrations (0.5% and 1% vol/vol) as a scattering agent. The phantoms were cooled overnight at 4°C, and then imaged on a Solaris preclinical surgical imaging system (PerkinElmer, Inc, Waltham, Massachusetts) using the 750 nm channel. Regions of interest (ROIs) were created to encompass the center region of the well, and the average fluorescence intensity per pixel was determined in Fiji software (ImageJ v1.51j),<sup>48-50</sup> then normalized to the highest muscle value (1% intralipid, 2% blood).

### Naive Mouse Study

All procedures were performed in accordance with protocols and standard operating procedures approved by the Institutional Animal Care and Use Committee at Dartmouth College. Female nude mice (6 weeks old, Charles River Laboratories, Inc, Wilmington, Massachusetts) were placed on a chlorophyll-free diet (Purified Mouse Diet; MP Biomedicals, LLC, Illkirch, France) for a minimum of three days in order to reduce the effects of autofluorescence. Previous studies, as well as unpublished data from our laboratory, have confirmed binding of ABY-029, an anti-EGFR Affibody-IRDye 800CW conjugate, to murine EGFR.<sup>51,52</sup> A 1:1 mixture of ABY-029 and IRDye 700DX carboxylate, the latter acting as a nonspecific perfusion agent to control for any observed EGFR binding in these normal tissues, was injected (4.98  $\mu$ M, 200  $\mu$ L) into the tail vein under light isoflurane anesthesia (1%-2% isoflurane, 1 L/min O<sub>2</sub>). At 1- and 2-hour time points, mice were anesthetized and then killed by cervical dislocation followed by diaphragmatic puncture. Tissue was removed from the right and left flanks of 2 mice at both the 1- and 2-hour time points ( $n = 4$ , per time point). Right and left flanks from an additional control mouse ( $n = 2$ ) were processed in a similar manner but did not receive injection of the fluorescent agents. Muscle, fascia, sciatic nerve, and fat were excised from each flank and utilized for ex vivo fluorescence analysis. The tissues were placed on a glass slide and imaged on three preclinical fluorescence systems: (1) Solaris (PerkinElmer)—a broad-beam, open-air surgical system, (2) Pearl (LI-COR Biosciences, Inc)—a broad-beam, black box system, and (3) Odyssey (LI-COR Biosciences, Inc)—a black box, flatbed scanning system. Ex vivo fluorescence data were analyzed using Fiji<sup>48-50</sup> by creating ROIs around the tissues of interest in each of the images produced by the Solaris, Pearl, and Odyssey imaging systems. Fluorescence signal was normalized to the muscle tissue for each time point and imaging system. Muscle was used as a reference tissue because it is known to be devoid of EGFR. In the absence of EGFR, ABY-029, and IRDye 700DX, carboxylate should demonstrate identical pharmacokinetics, thus normalizing fluorescence signal between imaging systems, time points, and tissue types. This method has previously been used successfully as a control for ABY-029 and other EGFR-targeted imaging agents.<sup>42-44</sup>

### Surgical Phantoms

Large cylindrical phantoms (11 cm diameter, 6 cm height) were created with a 16.4 cm<sup>3</sup> tumor-simulating inclusion at approximately 2 cm depth. Both the inclusion and background phantoms were made with 1% (vol/vol) blood and 1% (vol/vol) intralipid to best represent general connective tissue. First, in order to test the inclusion fluorescence, ABY-029 concentration was varied (125, 500, and 1000 ng/mL) while the background tissue remained free of fluorophore. Second, the TBR was studied by holding the ABY-029 concentration in the inclusion at 500 ng/mL and varying the background

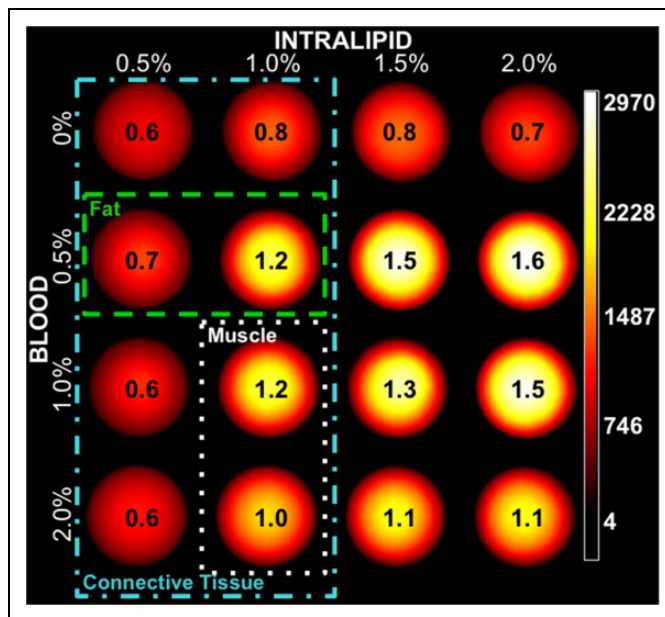


**Figure 2.** Gelatin phantoms demonstrate the effects of normal connective tissue optical properties on ABY-029 fluorescence. Each well held a constant concentration of ABY-029 (50 nM). The concentration of blood was varied in the rows, and the concentration of intralipid was varied in the columns. The wells with the optical properties best representing general connective tissue, fat, and muscle are shown.<sup>45-47</sup> The value in the center of each well is the average fluorescence normalized to the muscle values best represented by mouse muscle (1% intralipid, 2% blood).

concentration (50, 100, 166.7, 250, and 500 ng/mL) such that the effective TBR would be 10:1, 5:1, 3:1, 2:1, and 1:1, respectively. A blinded orthopedic oncology surgeon then attempted to locate each inclusion by using a Solaris imager to display fluorescence intensity over the surface of the phantom. Using prior knowledge of the inclusion volume, surgical cuts were made to the phantom, beginning on the outermost aspects and progressing inwards, in order to decrease the tissue-mimicking margins to approximately 1 cm. The stopping criteria were (1) an expected volume of the phantom was left (16.4 cm<sup>3</sup> + 1 cm margins), with fairly even fluorescence signal on all six sides, or (2) the inclusion was cut into. If a surgical incision was made into the inclusion, this was considered a failed experiment, and no margin thickness was recorded. The remaining cuboid was cut horizontally and vertically through the center and each section imaged next to a ruler. The margin thickness was analyzed using Fiji software<sup>48-50</sup> and plotted against mean fluorescence for the varying inclusion ABY-029 concentrations and TBRs.

### Results and Discussion

The presence of light absorbing and scattering agents in a medium or tissue can greatly affect the observed emission intensity of a given fluorophore. Although these effects are reduced in the near-infrared region, as compared to the visible wavelengths, they are not negligible. Here, we tested the effects

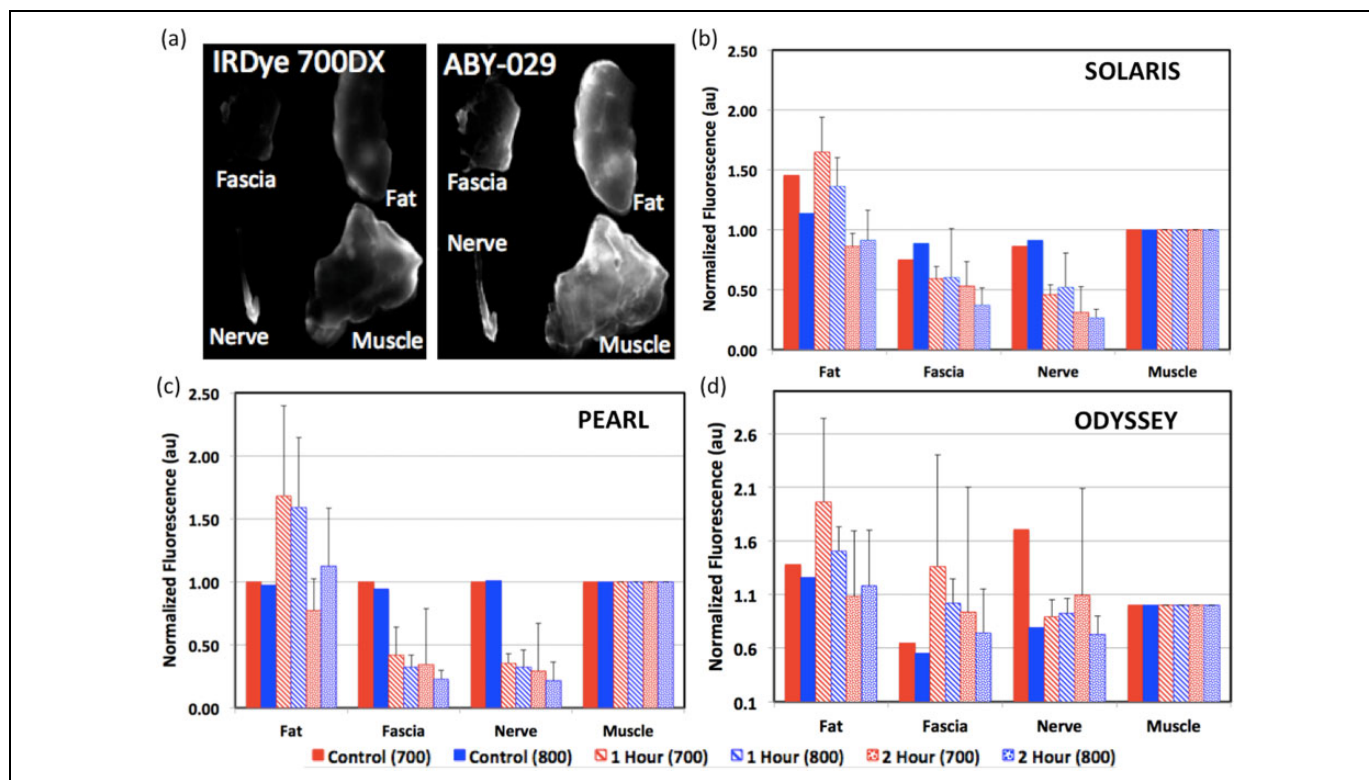


**Figure 3.** A, Uptake of ABY-029 and IRDye 700DX in ex vivo naive mouse tissues. Images are nonnormalized to demonstrate the different optical properties of the fluorophores. Fluorescence intensity, normalized to muscle, is compared for three imaging systems: (B) Solaris (PerkinElmer)—broad beam, open-air (660 and 750 nm channels), (C) Pearl (LI-COR Biosciences, Inc)—broad beam, closed box (700 and 800 nm channels), and (D) Odyssey (LI-COR Biosciences, Inc)—flatbed, scanning (700 and 800 nm channels). In general, control tissues demonstrated similar autofluorescence to muscle tissue. No differences were observed between the epidermal growth factor receptor (EGFR)-targeted fluorophore ABY-029 (800 nm channel) and the perfusion agent control IRDye 700DX (700 nm channel). Observed fluorescence is most stable in the broad beam fluorescence systems (Solaris and Pearl), while the Odyssey scanning system is more prone to large variations in signal over time, likely due to high surface weighting and less tissue-volume averaging. Values reported as mean (standard deviation [SD]).

of light-absorbing (blood; 0.5%, 1%, and 2%) and scattering (intralipid; 0.5% and 1%) media in biologically relevant concentrations on the observed fluorescence of a constant ABY-029 concentration (50 nM).<sup>45-47</sup> As demonstrated in Figure 2, ABY-029 fluorescence increases proportionally with scattering agents and decreases proportionally with absorbing agents. Since muscle and fat are the most common normal tissues to be associated with soft-tissue sarcomas, the range of absorbing and scattering parameters of these tissues<sup>45-47</sup> is highlighted.

The simulation accuracy of these tissue-mimicking phantoms was tested by administering ABY-029 to naive mice and observing effective fluorescence intensities in normal tissues at 1 and 2 hours postadministration. Normalized fluorescence values for each fluorescence system can be observed in Figure 3. In general, tissues from the control mouse all had similar autofluorescence signal to the muscle tissue. In the experimental mice, there were no differences observed between ABY-029 and IRDye 700DX carboxylate for each imaging system, time point, and tissue type, indicating that ABY-029 binding to native EGFR in these naive tissues was not contributing to the accumulation or retention of the targeted agent. These data suggest that the EGFR-targeted fluorophore ABY-029 may

be utilized to preferentially visualize EGFR-positive sarcoma tumors over the surrounding naive tissues. The exception to this was in the nerve tissue of the control mouse when scanned on the Odyssey, where the fluorescence signal in the 700-nm channel was over 2x that in the 800-nm channel. However, this effect of autofluorescence and control nerve variance was only observed in the Odyssey, and therefore, these effects are likely artifacts of the surface-weighted imaging in this system and a result of having only a single set of control tissues. Such effects were not observed in the Solaris or Pearl systems and thus would not affect fluorescence signal in the clinical context. Investigation is currently underway in our laboratory to evaluate the ability of ABY-029 to label EGFR-positive sarcoma tumors in a murine model.

Comparing ABY-029 fluorescence in gelatin phantoms (Figure 2) to that of naive mice connective tissues (Figure 3) indicates that the phantoms accurately represent the range of fluorescence that will be observed in normal tissues. At short time periods (1 hour), the fluorescence intensity of ABY-029 in normal mouse fat, fascia, and nerve varied from 0.3 to 2× that of muscle. The gelatin phantoms displayed maximal contrast ratios of 0.6 to 1.6× that of the muscle condition with the

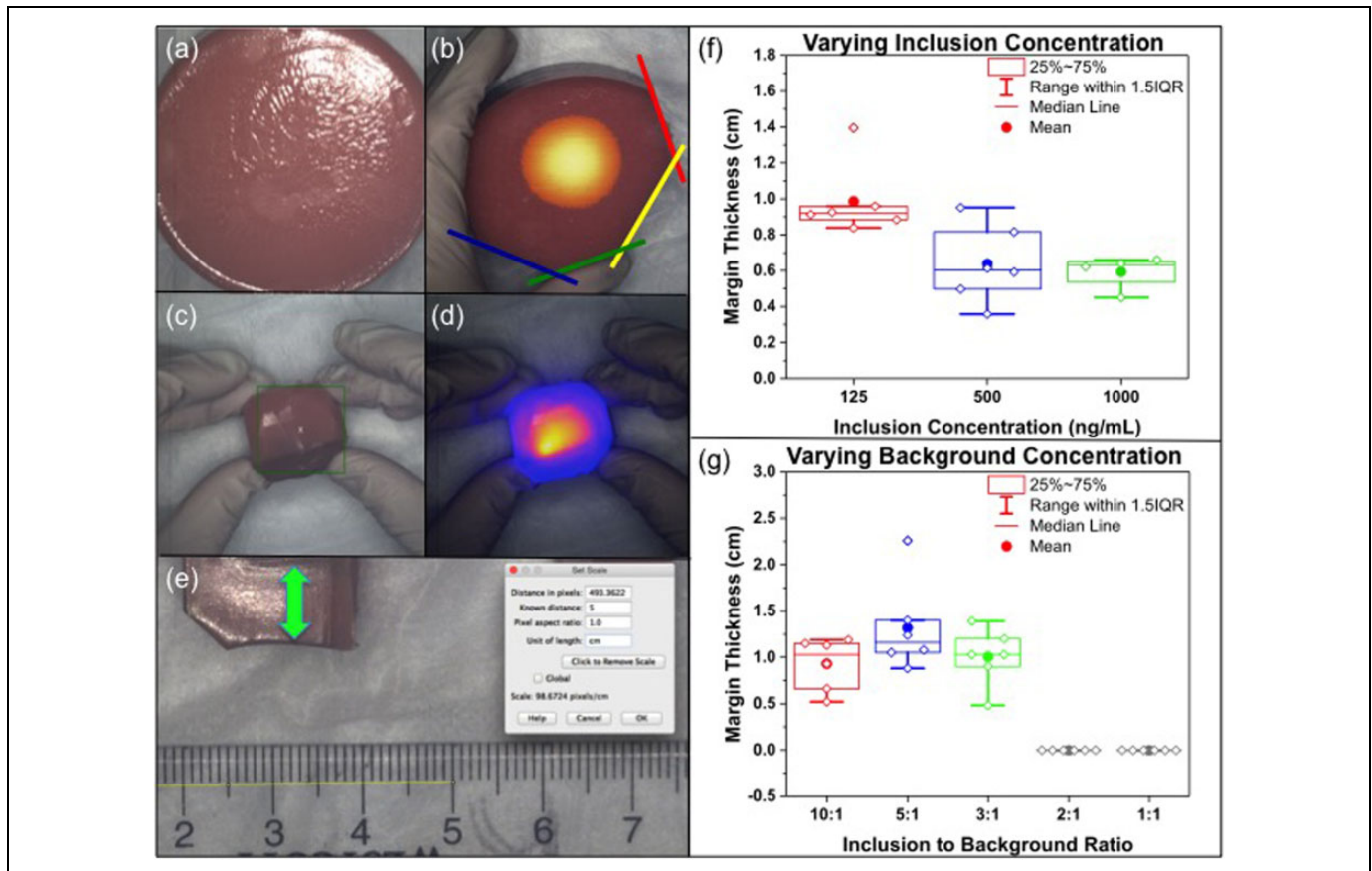


**Figure 4.** Surgical phantoms for assessing surgical resection margin utilizing a Solaris imager to display indirect fluorescence. Inclusion and background were made with 10% (wt/vol) gelatin, 1% (vol/vol) blood, and 1% (vol/vol) intralipid, and the levels of ABY-029 were varied. A, Photograph of the surface of the surgical phantom (11 cm diameter and 6 cm height). B, Fluorescence from the 16.4 cm<sup>3</sup> fluorescent inclusion overlaid on a white light photograph. The colored lines indicate cut lines as the boundary of the inclusion is gradually approached. The resulting inclusion with ~1 cm margins as a white light image (C) and fluorescence overlay (D). E, The inclusion was bisected and the margin distance assessed manually using Fiji.<sup>48-50</sup> F, The margin assessment of inclusions with varying concentrations of ABY-029 and nonfluorescent background. G, The margin assessment with constant ABY-029 concentration in the inclusion (500 ng/mL), and varying ABY-029 concentration in the background to achieve 10:1, 5:1, 3:1, 2:1, and 1:1 inclusion-to-background ratios.

highest absorption and scatter properties (1% intralipid, 2% blood condition). These data indicate that the commonly encountered tissues in sarcoma surgery, namely muscle, fat, fascia, and nerve can be accurately represented in phantom models, and therefore, such models could be utilized to further investigate indirect fluorescence for sarcoma resection.

Large-scale surgical phantoms were made to study the effect of ABY-029 inclusion concentration and TBR on our ability to surgically excise a sarcoma tumor using indirect fluorescence (Figure 4A-E). Using the gelatin well phantoms and the naive mouse tissues as guidelines for normal connective tissue optical properties, the surgical phantoms were made using moderate scatter and absorption conditions (1% intralipid and 1% blood). We demonstrated that a surgeon, blinded to the location of the inclusion, could excise the inclusion with a reasonable margin (~1 cm) for all inclusion concentrations tested (Figure 4F) and with TBRs ranging from 10:1 to 3:1 (Figure 4G). Surgical margins around the inclusion with TBRs of 2:1 and 1:1 were not achievable due to the lack of fluorescence

contrast; these ratios resulted in cuts into the inclusion and were considered a failed experiment. Therefore, we can conclude that a TBR of at least 3:1 is likely required to be able to perform sarcoma resection using indirect fluorescence guidance. Still, more extensive phantoms and sarcoma-bearing mice will need to be tested to further validate the depth of imaging, optimal ABY-029 dose, and timing from ABY-029 administration to surgery.

## Conclusion

Fluorescence guidance has proven effective for enhancing the accuracy of cancer surgery where the tumor is viewed directly and removal of the normal surrounding tissue, such as in the brain, may be harmful to the patient. However, many other cancer types require wide local excision with the goal of negative margins for cure. In these cases, the use of fluorescence to monitor tumor location and margin thickness is likely possible but would require more complex accounting for marginal tissue



and tumor volume, optical characteristics, and excitatory signal strength. Our preliminary investigation demonstrates that the tissue-mimicking phantoms accurately simulate the optical properties of naive mouse connective tissues with the use of ABY-029. Furthermore, our naive mouse experiment suggests that ABY-029 may be effective in distinguishing EGFR-positive sarcoma tumors within their surrounding tissues after intravascular clearance of the EGFR-targeted probe. Finally, a TBR of 3:1 is likely the minimum ratio necessary for successful excision of a tumor with clear margins. Near-infrared fluorescence is a promising tool for indirect, subsurface visualization of tumors requiring surgical resection by wide local excision, and further investigation should continue to delineate the properties of ABY-029 and other targeted probes in naive and tumor tissues.

### Acknowledgment

The authors thank G. Douglas Letson (Moffitt Cancer Center, Tampa, Florida) for the intraoperative images.

### Declaration of Conflicting Interests

The author(s) declared the following potential conflicts of interest with respect to the research, authorship, and/or publication of this article: No significant relationship exists between the authors and the companies/organizations whose products or services may be referenced in this article, with the exception of Dr Feldwisch who is an Affibody AB employee and Affibody AB stockholder. In addition, Dr Feldwisch has a patent WO2009080811 (A1) pending.

### Funding

The author(s) disclosed receipt of the following financial support for the research, authorship, and/or publication of this article: This work was funded by the Orthopaedic Research and Education Foundation (grant number 16-014) and the National Institutes of Health (grant number R01CA167413). JTE is supported by a NIH/NCI K99 grant (grant number 1K99CA190890).

### References

1. Tipirneni KE, Warram JM, Moore LS, et al. Oncologic procedures amenable to fluorescence-guided surgery. *Ann Surg.* 2017; 266(1):36-47. doi:10.1097/SLA.0000000000002127.
2. Stummer W, Pichlmeier U, Meinel T, Wiestler OD, Zanella F, Reulen HJ. Fluorescence-guided surgery with 5-aminolevulinic acid for resection of malignant glioma: a randomised controlled multicentre phase III trial. *Lancet Oncol.* 2006;7(5):392-401. doi: 10.1016/S1470-2045(06)70665-9.
3. Valdés PA, Leblond F, Kim A, et al. Quantitative fluorescence in intracranial tumor: implications for ALA-induced PpIX as an intraoperative biomarker. *J Neurosurg.* 2011;115(1):11-17. doi: 10.3171/2011.2.JNS101451.
4. Mansouri A, Mansouri S, Hachem LD, et al. The role of 5-aminolevulinic acid in enhancing surgery for high-grade glioma, its current boundaries, and future perspectives: a systematic review. *Cancer.* 2016;122(16):2469-2478. doi:10.1002/cncr.30088.
5. Butte PV, Mamelak A, Parrish-Novak J, et al. Near-infrared imaging of brain tumors using the tumor paint BLZ-100 to achieve near-complete resection of brain tumors. *Neurosurg Focus.* 2014; 36(2):E1. doi:10.3171/2013.11.FOCUS13497.
6. Pan Y, Volkmer J-P, Mach KE, et al. Endoscopic molecular imaging of human bladder cancer using a CD47 antibody. *Sci Transl Med.* 2014;6(260):260ra148. doi:10.1126/scitranslmed.3009457.
7. Stenzl A, Burger M, Fradet Y, et al. Hexaminolevulinate-guided fluorescence cystoscopy reduces recurrence in patients with non-muscle invasive bladder cancer. *J Urol.* 2010;184(5):1907-1913. doi:10.1016/j.juro.2010.06.148.
8. Grossman HB, Stenzl A, Fradet Y, et al. Long-term decrease in bladder cancer recurrence with hexaminolevulinate enabled fluorescence cystoscopy. *J Urol.* 2012;188(1):58-62. doi:10.1016/j.juro.2012.03.007.
9. Rosenthal EL, Warram JM, de Boer E, et al. Safety and tumor specificity of cetuximab-IRDye800 for surgical navigation in head and neck cancer. *Clin Cancer Res.* 2015;21(16): 3658-3666. doi:10.1158/1078-0432.CCR-14-3284.
10. Atallah I, Milet C, Coll J-L, Rey E, Righini CA, Hurbin A. Role of near-infrared fluorescence imaging in head and neck cancer surgery: from animal models to humans. *Eur Arch Otorhinolaryngol.* 2015;272(10):2593-2600. doi:10.1007/s00405-014-3224-y.
11. Potter BK, Hwang PF, Forsberg JA, et al. Impact of margin status and local recurrence on soft-tissue sarcoma outcomes. *J Bone Joint Surg Am.* 2013;95(20):e151. doi:10.2106/JBJS.L.01149.
12. Stojadinovic A, Leung DHY, Hoos A, Jaques DP, Lewis JJ, Brennan MF. Analysis of the prognostic significance of microscopic margins in 2,084 localized primary adult soft tissue sarcomas. *Ann Surg.* 2002;235(3):424-434. doi:10.1097/00000658-200203000-00015.
13. Pisters PW, Leung DHY, Woodruff J, Shi W, Brennan MF. Analysis of prognostic factors in 1,041 patients with localized soft tissue sarcomas of the extremities. *J Clin Oncol.* 1996;14(5): 1679-1689. doi:10.1200/jco.1996.14.5.1679.
14. Stahl JM, Corso CD, Park HS, et al. The effect of microscopic margin status on survival in adult retroperitoneal soft tissue sarcomas. *Eur J Surg Oncol.* 2017;43(1):168-174. doi:10.1016/j.ejso.2016.05.031.
15. Moore GE, Peyton WT, French LA, Walker WW. The clinical use of fluorescein in neurosurgery: the localization of brain tumors. *J Neurosurg.* 1948;5(4):392-398. doi:10.3171/jns.1948.5.4.0392.
16. Kim A, Khurana M, Moriyama Y, Wilson BC. Quantification of in vivo fluorescence decoupled from the effects of tissue optical properties using fiber-optic spectroscopy measurements. *J Biomed Opt.* 2010;15(6):67006. doi:10.1117/1.3523616.
17. Valdés PA, Leblond F, Jacobs VL, Wilson BC, Paulsen KD, Roberts DW. Quantitative, spectrally-resolved intraoperative fluorescence imaging. *Sci Rep.* 2012;2:798. doi:10.1038/srep00798.
18. Elliott JT, Evans LT, Bravo JJ, et al. Corticosteroid therapy modifies fluorescence surgery contrast in preclinical and clinical brain cancer. Manuscript in Preparation.
19. Marshall MV, Draney D, Sevic-Muraca EM, Olive DM. Single-dose intravenous toxicity study of IRDye 800CW in Sprague-Dawley rats. *Mol Imaging Biol.* 2010;12(6):583-594. doi:10.1007/s11307-010-0317-x.

20. Samkoe KS, Gunn JR, Marra K, et al. Toxicity and pharmacokinetic profile for single-dose injection of ABY-029: a fluorescent anti-EGFR synthetic Affibody molecule for human use. *Mol Imaging Biol.* 2017;19(4):512-521. doi:10.1007/s11307-016-1033-y.
21. Pogue BW, Paulsen KD, Hull SM, et al. Advancing molecular-guided surgery through probe development and testing in a moderate cost evaluation pipeline. *Proc SPIE.* 2015;9311. doi:10.1117/12.2083224.
22. Fidel J, Kennedy KC, Dernell WS, et al. Preclinical validation of the utility of BLZ-100 in providing fluorescence contrast for imaging spontaneous solid tumors. *Cancer Res.* 2015;75(20):4283-4291. doi:10.1158/0008-5472.CAN-15-0471.
23. Parrish-Novak J, Byrnes-Blake K, Lalayeva N, et al. Nonclinical profile of BLZ-100, a tumor-targeting fluorescent imaging agent. *Int J Toxicol.* 2017;36(2):104-112. doi:10.1177/1091581817697685.
24. Sexton K, Tichauer K, Samkoe KS, Gunn J, Hoopes PJ, Pogue BW. Fluorescent Affibody peptide penetration in glioma margin is superior to full antibody. *PLoS One.* 2013;8(4):e60390. doi:10.1371/journal.pone.0060390.
25. Elliott JT, Dsouza AV, Marra K, Pogue BW, Roberts DW, Paulsen KD. Microdose fluorescence imaging of ABY-029 on an operating microscope adapted by custom illumination and imaging modules. *Biomed Opt Express.* 2016;7(9):3280-3288. doi:10.1364/BOE.7.003280.
26. de Souza ALR, Marra K, Gunn J, et al. Fluorescent Affibody molecule administered in vivo at a microdose level labels EGFR expressing glioma tumor regions. *Mol Imaging Biol.* 2017;19:41-48. doi:10.1007/s11307-016-0980-7.
27. Elliott JT, Marra K, Evans LT, et al. Simultaneous in vivo fluorescent markers for perfusion, protoporphyrin metabolism, and EGFR expression for optically guided identification of orthotopic glioma. *Clin Cancer Res.* 2017;23(9):2203-2212. doi:10.1158/1078-0432.CCR-16-1400.
28. Hinni ML, Ferlito A, Brandwein-Gensler MS, et al. Adult height and head and neck cancer: a pooled analysis within the INHANCE consortium. *Head Neck.* 2013;35:1362-1370. doi:10.1002/HED.
29. Rosenthal EL, Kulbersh BD, Duncan RD, et al. In vivo detection of head and neck cancer orthotopic xenografts by immunofluorescence. *Laryngoscope.* 2006;116(9):1636-1641. doi:10.1097/01.mlg.0000232513.19873.da.
30. Rosenthal EL, Kulbersh BD, King T, Chaudhuri TR, Zinn KR. Use of fluorescent labeled anti-epidermal growth factor receptor antibody to image head and neck squamous cell carcinoma xenografts. *Mol Cancer Ther.* 2007;6(4):1230-1238. doi:10.1158/1535-7163.MCT-06-0741.
31. Gleysteen JP, Newman JR, Chhieng D, Frost A, Zinn KR, Rosenthal EL. Fluorescent labeled anti-EGFR antibody for identification of regional and distant metastasis in a preclinical xenograft model. *Head Neck.* 2008;30(6):782-789. doi:10.1002/HED.20782.
32. Heath CH, Deep NL, Sweeny L, Zinn KR, Rosenthal EL. Use of panitumumab-IRDye800 to image microscopic head and neck cancer in an orthotopic surgical model. *Ann Surg Oncol.* 2012;19(12):3879-3887. doi:10.1245/s10434-012-2435-y.
33. Day KE, Sweeny L, Kulbersh B, Zinn KR, Rosenthal EL. Preclinical comparison of near-infrared-labeled cetuximab and panitumumab for optical imaging of head and neck squamous cell carcinoma. *Mol Imaging Biol.* 2013;15(6):722-729. doi:10.1007/s11307-013-0652-9.
34. Gong H, Kovar JL, Cheung L, Rosenthal EL, Olive DM. A comparative study of Affibody, panitumumab, and EGF for near-infrared fluorescence imaging of EGFR- and EGFRvIII-expressing tumors. *Cancer Biol Ther.* 2014;15(2):185-193. doi:10.4161/cbt.26719.
35. Moore LS, Rosenthal EL, de Boer E, et al. Effects of an unlabeled loading dose on tumor-specific uptake of a fluorescently labeled antibody for optical surgical navigation. *Mol Imaging Biol.* 2017;19(4):610-616. doi:10.1007/s11307-016-1022-1.
36. Mito JK, Ferrer JM, Brigman BE, et al. Intraoperative detection and removal of microscopic residual sarcoma using wide-field imaging. *Cancer.* 2012;118(21):5320-5330. doi:10.1002/cncr.27458.
37. Whitley MJ, Cardona DM, Lazarides AL, et al. A mouse-human phase 1 co-clinical trial of a protease-activated fluorescent probe for imaging cancer. *Sci Transl Med.* 2016;8(320):320ra4. doi:10.1126/scitranslmed.aad0293.
38. Miwa S, Hiroshima Y, Yano S, et al. Fluorescence-guided surgery improves outcome in an orthotopic osteosarcoma nude-mouse model. *J Orthop Res.* 2014;32(12):1596-1601. doi:10.1002/jor.22706.
39. Uehara F, Hiroshima Y, Miwa S, et al. Fluorescence-guided surgery of retroperitoneal-implanted human fibrosarcoma in nude mice delays or eliminates tumor recurrence and increases survival compared to bright-light surgery. *PLoS One.* 2015;10(2):e0116865. doi:10.1371/journal.pone.0116865.
40. Yano S, Miwa S, Kishimoto H, et al. Targeting tumors with a killer-reporter adenovirus for curative fluorescence-guided surgery of soft-tissue sarcoma. *Oncotarget.* 2015;6(15):13133-13148. doi:10.18632/oncotarget.3811.
41. Yano S, Miwa S, Kishimoto H, et al. Eradication of osteosarcoma by fluorescence-guided surgery with tumor labeling by a killer-reporter adenovirus. *J Orthop Res.* 2016;34(5):836-844. doi:10.1002/jor.23073.
42. Samkoe KS, Tichauer KM, Gunn JR, Wells WA, Hasan T, Pogue BW. Quantitative in vivo immunohistochemistry of epidermal growth factor receptor using a receptor concentration imaging approach. *Cancer Res.* 2014;74(24):7465-7474. doi:10.1158/0008-5472.CAN-14-0141.
43. Davis SC, Gibbs SL, Gunn JR, Pogue BW. Topical dual-stain difference imaging for rapid intra-operative tumor identification in fresh specimens. *Opt Lett.* 2013;38(23):5184-5187.
44. Tichauer KM, Samkoe KS, Sexton KJ, et al. In vivo quantification of tumor receptor binding potential with dual-reporter molecular imaging. *Mol Imaging Biol.* 2012;14(5):584-592. doi:10.1007/s11307-011-0534-y.
45. Pogue BW, Patterson MS. Review of tissue simulating phantoms for optical spectroscopy, imaging and dosimetry. *J Biomed Opt.* 2006;11(4):41102. doi:10.1117/1.2335429.
46. Jacques SL. Optical properties of biological tissues: a review. *Phys Med Biol.* 2013;58(14):R37-R61. doi:10.1088/0031-9155/58/14/5007.

47. Srinivasan S, Pogue BW, Jiang S, et al. Interpreting hemoglobin and water concentration, oxygen saturation, and scattering measured in vivo by near-infrared breast tomography. *Proc Natl Acad Sci*. 2003;100(21):12349-12354. doi:10.1073/pnas.2032822100.
48. Schneider CA, Rasband WS, Eliceiri KW. NIH image to ImageJ: 25 years of image analysis. *Nat Methods*. 2012;9(7):671-675. doi:10.1038/nmeth.2089.
49. Schindelin J, Arganda-Carreras I, Frise E, et al. Fiji: an open-source platform for biological-image analysis. *Nat Methods*. 2012;9(7):676-682. doi:10.1038/nmeth.2019.
50. Schindelin J, Rueden CT, Hiner MC, Eliceiri KW. The ImageJ ecosystem: an open platform for biomedical image analysis. *Mol Reprod Dev*. 2015;82(7-8):518-529. doi:10.1002/mrd.22489.
51. Friedman M, Orlova A, Johansson E, et al. Directed evolution to low nanomolar affinity of a tumor-targeting epidermal growth factor receptor-binding Affibody molecule. *J Mol Biol*. 2008;376(5):1388-1402. doi:10.1016/j.jmb.2007.12.060.
52. Frejd FY, Kim K-T. Affibody molecules as engineered protein drugs. *Exp Mol Med*. 2017;49(3):e306. doi:10.1038/emmm.2017.35.